A Channel Estimation Scheme for Analog Network Coding based on OFDM in a Multipath Fading Environment

Tomas Sjödin

December 3, 2009
Master's Thesis in Computing Science, 30 ECTS-credits
Supervisor at CS-UmU: Jerry Eriksson
Examiner: Per Lindström

Umeå University
Department of Computing Science
SE-901 87 UMEÅ
SWEDEN

Abstract

The capacity of future wireless networks must be increased to accommodate more demanding wireless devices and applications. Network coding at the physical layer, although originally applied in wired networks, can be used to exploit the broadcasting capability of the wireless channel to increase network capacity. A wireless channel is characterized by multipath fading which produces interference and distorts the transmitted signal. Recently, broadband analog network coding (ANC) was proposed to cope with multipath fading assuming full knowledge of the channel state information (CSI). However, broadband ANC requires accurate channel estimation (CE) for self-information removal and signal recovery.

In this thesis, we propose a two-stage pilot-assisted CE scheme for broadband ANC based on orthogonal frequency division multiplexing (OFDM) radio access. The proposed CE scheme is divided into two stages. During the first stage the users transmit their pilot signals to the relay which estimates the both CSIs from the interfered signal, and during the second stage the relay broadcast its pilot signal to the users which estimates the corresponding CSI. The CE at the relay during the first stage is possible because the pilot signals transmitted by the users are designed to avoid pilot interference and consequently, allow the relay to estimate the CSIs from both users.

It was shown by computer simulation that, even with imperfect CSI, the bit-error-rate performance of broadband ANC gives a satisfactory performance for a low and moderate mobile terminal speed in a multipath fading channel.

Abbreviations

$f_D T_s$	Normalized maximum Doppler frequency
ANC	Analog network coding
AWGN	Additive white Gaussian noise
BER	Bit-error-rate
CE	Channel estimation
CSI	Channel state information
DFT	Discrete Fourier transform
FDE	Frequency-domain equalization
FFT	Fast Fourier transform
GI	Guard interval
IDFT	Inverse discrete Fourier transform
IFFT	Inverse fast Fourier transform
ISI	Intersymbol interference
MISO	Multiple-input single-output
OFDM	Orthogonal frequency division multiplexing
QPSK	Quadrature phase shift keying
SISO	Single-input single-output
TWRN	Two-way relay network
ZF	Zero forcing

Contents

List of Figures

Chapter 1

Introduction

More and more competent mobile devices are made available to the public every day, which allows for implementation of advanced applications that requires high capacity wireless networks. This development will ultimately lead to the need of new wireless networks which can provide higher capacity than today's networks. Network coding was first used in wired networks to increase network capacity [2]. This gain in network capacity can also be achieved in wireless networks by applying the principle of network coding which exploits the natural broadcasting capability of the wireless medium [3], [4]. The work introduced in [5] and [6] takes the concept of network coding even further and show that network coding at the physical layer (PNC), where the users signals are mixed in the wireless medium, can double the network capacity of bi-directional wireless communication. The exchange of data between the users in a PNC network is divided into two stages. During the first stage the users transmit to the relay, and during the second stage the relay decode-and-forward the received signal to the users.

1.1 Analog Network Coding

Narrowband analog network coding (ANC) introduced in [7] is a less complex implementation of PNC, where the relay uses a simple amplify-and-forward protocol. Broadband communications over a wireless channel does however experience multipath fading which distorts the transmitted signal. Recently, broadband ANC based on orthogonal frequency domain multiplexing (OFDM) was introduced with the assumption of perfect knowledge of the channel state information (CSI) between the users and the relay terminal [8]. However, the signal recovery process in broadband ANC networks require accurate channel estimation (CE).

1.2 Problem Description

In conventional (without relay) and cooperative (with relay) networks the signals transmitted from different users are always separated in time or frequency to avoid interference. This is however not the case in an ANC network where users' signals are transmitted at the same time. Hence, in the case of a pilot signal transmission, the relay will receive an interfered pilot signal from the users. This render the system unable to use conventional pilot-assisted CE methods to estimate the CSIs in two stages, and thus, the capacity benefits of ANC cannot be maintained. Conventional CE methods could however be used in broadband ANC networks, but would introduce two important problems:

– Four stages would be needed to estimate the CSIs in an ANC network to separate different user's pilot signals [9]. This would significantly degrade the capacity benefit of the ANC scheme since two extra stages will be required to perform pilot-assisted CE.

– To avoid interfering pilot signals in conventional (without relay) and cooperative (relay) networks, the different users' pilot signals are separated by orthogonal frequencies or different time slots [9],[10]. In broadband ANC, the users are however allowed to transmit simultaneously during the first stage, which results in interfering pilot signals (CSIs will overlap each other). Consequently, the relay cannot estimate the CSIs from different users during the first pilot transmission stage.

1.3 Goal

The goal of this thesis is to develop a pilot-assisted CE scheme, suited for broadband ANC. A CE scheme for ANC cannot use more than two stages to estimate all wireless channels in the network to utilize the capacity benefits of ANC. The main problem is to estimate two CSIs at the relay from one received signal during the first stage. The proposed solution to the problem is described in Chapter 4.

1.4 The Proposed Solution

The pilot-assisted CE scheme for broadband ANC presented in this work consists of two stages. During the first stage, the users transmit their pilot signals to the relay simultaneously. One of the users' pilot signal is cyclically shifted, which makes it possible for the relay to separate and estimate the CSIs from both users using the interfered received signal [11]. The first stage is named multiple-input single-output channel estimation (MISO-CE) because of its analogy to multiple-input multiple-output (MIMO) systems. The second stage is used by the relay to broadcast its pilot signal to the users. By using the pilot signal from the relay, both users can estimate the corresponding CSI.

1.5 Related Work

In [12], a complex maximum likelihood (ML) CE is presented for narrowband (i.e, frequency-nonselective fading) ANC, which requires knowledge of the noise variance and the channel cross-correlation coefficients.

1.6 Professor F. Adachi's Laboratory

In early October 2008 I left Sweden to study abroad at Tohoku university in Sendai Japan. I was assigned to Professor F. Adachi's laboratory where they conduct research concerning wireless communication [13]. Professor Adachi was also my academic advisor during my one year stay at Tohoku University. I was determined to do my master's thesis during my year in Japan and after some time I started working with Dr. H. Gacanin who is an expert in digital signal transmission. Dr. Gacanin suggested a research topic about channel estimation in an analog network coding network and after discussions with Processor Adachi we decided that this was a good topic.

1.7 A collaboration based work

This thesis is based on the work I did, during my year in Professor F. Adachi's laboratory at Tohoku University, Sendai, Japan, in collaboration with Dr. H. Gacanin. The results of our work is originally presented in a paper submitted to VTC2010-Spring [14]. The paper was still undergoing the reviewing process when this report was written.

1.8 Thesis Outline

The reminder of this thesis is organized as follows. Chapter 2 introduces important wireless communication concepts related to this work. A detailed description of the ANC network model is described in Chapter 3. Chapter 4 presents the proposed pilot-assisted CE scheme for broadband ANC. Computer simulations results are presented in Chapter 5. Chapter 6 concludes our findings. And finally, people who help making this project possible are acknowledged in Chapter 7.

Chapter 2

Wireless Communication

The purpose of this chapter is to give the reader a basic understanding of a few important concepts concerning wireless communication and the techniques that the work presented in this thesis is based on.

2.1 Signal Theory

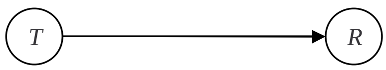

Figure 2.1: A simple transmitter/receiver network, where user T wants to transmit to user R.

Consider the network illustrated in Fig. 2.1 consisting of the transmitting user T and the receiving user R, where user T wants to send a sequence of data to user R. To do so user T has to create a signal which is a physical representation of the data sequence. The type of signals used in wireless networks is typically periodic signals, where sine waves are used as carriers generally represented as a function of time t as

$$x(t) = A \cdot \cos(2\pi f t + \theta), \tag{2.1}$$

where A, f and θ are the amplitude, the frequency and the phase shift, respectively. The period of the sine wave is defined as $T = 1/f$ [15]. Figure 2.2 illustrates a sine wave (solid line) and a sine wave shifted 90°(dotted line).

2.1.1 Data Modulation

Digital data (0 and 1) can be modulated as a sine wave with three different techniques; amplitude modulation, frequency modulation and phase modulation [16]. The technique used in this work is phase modulation called phase shift keying (PSK). As the name suggest, PSK changes the phase of the sine wave to represent the data bits. The simplest version of PSK is binary phase shift keying (BPSK), which can be used to represent one bit (0 or 1) each period of the sine wave as illustrated in Fig. 2.3 by shifting the sine wave 180°. The most commonly used PSK modulation scheme is quadrature phase shift keying (QPSK) which can modulate two bits per period by shifting the sine wave 45° (11), 135° (10), 225°

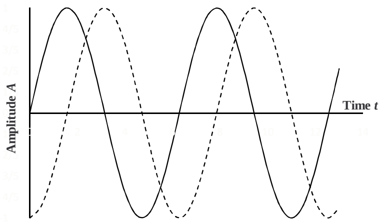

Figure 2.2: Time domain representation of a sinus wave (solid line) and a shifted sine wave (dotted line).

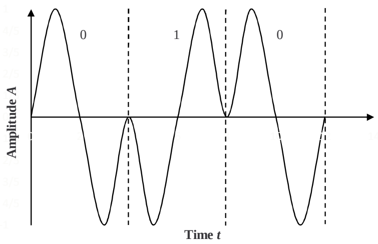

Figure 2.3: Binary phase shift keying modulation, where each period represents 0 or 1.

(00) or 315° (01). The advantage of a higher order PSK scheme like QPSK compared with BPSK is that the bit transmission rate becomes higher since two bits can be transmitted per period instead of one bit using the same bandwidth. Higher order PSK schemes are however more sensitive to interference than lower order schemes.

The modulated data signal sent by the transmitter must then be demodulated at the receiver to recover the data bits. This is done by comparing the received signal with a reference signal.

2.1.2 Frequency Domain

Equation (2.1) can be used to represent a signal in the time domain. A time domain signal can also be represented in the frequency domain, which is required to used certain techniques. I.e., this work uses a technique called zero forcing frequency domain equalization (ZF-FDE) (see Section 2.3.2), which is a used to recover a signal sent over a multipath fading channel (see Section 2.2).

Transforming a time domain signal into the frequency domain is equal to decomposing the signal into its sinusoidal frequency components [15]. The amplitude and phase of the frequency components can be represented as the complex numbers $\{X(n); n = 0 \sim N-1\}$. A discrete time domain signal $\{x(t); t = 0 \sim N-1\}$ can be transformed into the frequency domain signal $X(n)$ by a discrete Fourier transform (DFT) function defined as

$$X(n) = \sum_{t=0}^{N-1} x(t) \exp\left(-j2\pi n \frac{t}{N} \right) \tag{2.2}$$

for $n = 0 \sim N-1$. To transform $X(n)$ back to the time domain, the inverse discrete Fourier transform (IDFT) can be used as

$$x(t) = \frac{1}{N}\sum_{n=0}^{N-1} x(n)\exp\left(j2\pi n\frac{t}{N}\right) \tag{2.3}$$

for $t = 0 \sim N-1$. DFT and IDFT are however inefficient Fourier transform methods with the complexity $\bigcirc(N^2)$ because they do not exploit the symmetry and periodicity properties of the phase factor. A faster version of the DFT and IDFT are the fast Fourier transform (FFT) and inverse fast Fourier transform (IFFT), respectively, which produces the same result, but with lower complexity ($\bigcirc(N\log N)$) [17].

2.2 Multipath Fading

Figure 2.4: The signal sent through the wireless channel between the transmitter and receiver experience multipath fading.

When a signal is transmitted in a wireless network, it will normally propagate through several different paths because of reflection, diffraction and scattering on objects in the environment between the transmitter and the receiver. This results in several received instances of the transmitted signal at the receiver with different time delays. In other words, the transmitted signal is not equal to the received signal which is a big problem. This phenomena, illustrated in Fig. 2.4, is called multipath propagation which has the biggest impact on signal quality degradation [16].

The type of multipath propagation considered in this work is small-scale fading, which is characterized by a large number of paths and no line-of-sight (a typical big city environment) between the transmitter and the receiver. Small-scale fading is also known as Rayleigh fading because the envelope of the received signal can be described by the Rayleigh probability density function [18].

A number of techniques has been developed to overcome the system degrading effects of multipath fading. Section 2.3 and 2.4 introduce techniques used in this work to cope with multipath fading.

2.2.1 The Rayleigh Fading Model

The Rayleigh fading model can be used to simulate a wireless channel, which can be expressed as

$$h(k) = \frac{1}{\sqrt{L}}\sum_{l}^{L} \exp\left(j(2\pi \cdot f_D T \cdot k\cos\Phi_l + \phi_l)\right) \tag{2.4}$$

for $k = 0 \sim N$, where N, L, $f_D T$, Φ_n and ϕ_n are the number of samples (number of symbols that the transmitted signal consists of), the number of incoming waves, the normalized maximum Doppler frequency, the arrival angle of the nth incoming wave and the random phase of the received faded signal, respectively. $h(k)$ is called channel impulse response or path gain and is used later in Chapter 3 and 4. The normalized maximum Doppler frequency can be expressed as

$$f_D T = \frac{v}{\lambda} T, \tag{2.5}$$

where v is the speed of the mobile device relative to the transmitting antenna, $\lambda = c/f_c$ is the wave length of the transmitted wave (c is the speed of light and f_c is the carrier frequency) and T is the transmission data date. The Doppler frequency or Doppler shift is the change in frequency caused by the receiving antenna moving relative to the transmitting antenna [19].

2.2.2 Additive White Gaussian Noise

Another problem in wireless communications is the background noise added at the receiver due to natural causes such as the vibrations of atoms in the antennas. This is can be modeled with the additive white Gaussian noise (AWGN) channel model following the Gaussian probability distribution function [19]. The background noise is however considered as a lesser concern than the multipath fading as long as a good signal-to-noise ratio can be maintained.

2.3 Signal Recovery

Section 2.2 introduced the problem of multipath fading, which is a signal impairing phenomena in wireless network. In short, this result in a received signal at the receiver which is not equal to the transmitted signal. This is a big problem since the receiving terminal cannot recover the data transmitted by the transmitting terminal unless the received signal is equal or close to equal to the transmitted signal. A combination of two techniques that can be used to perform signal recovery is pilot-assisted channel estimation (CE) and zero forcing frequency domain equalization which is described next.

2.3.1 Pilot-assisted Channel Estimation

The CE technique considered in this work is pilot-assisted CE, where the main idea is to transmit a signal known by the receiver called a pilot signal. This approach makes it possible for the receiving terminal to estimate the channel impulse response (denoted $h(t)$) and/or the channel gain (denoted $H(n)$), where the channel impulse response and the channel gain are the estimation of the channel in the time domain and the frequency domain, respectively. If the time- or frequency domain estimation of the channel is needed depends on which kind of equalization technique that is used.

Consider the network shown in Fig. 2.1, where user T transmit to user R. As illustrated in Fig. 2.5, assume that user T transmit its pilot signal $p(t)$ to R (gray boxes) which uses $p(t)$ to estimate the channel. The channel estimate $h^e(t)$ is then used by R during the following N_b data transmissions (white boxes) to recover the transmitted signal. The channel estimation process presented in this thesis is described in Chapter 4.

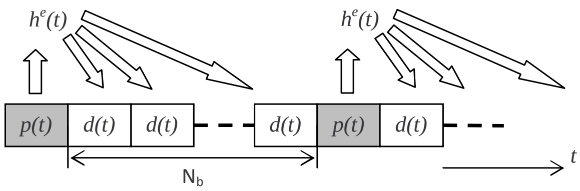

Figure 2.5: A pilot signal $p(t)$ is transmitted with an even interval to allow the receiver to obtain the channel estimate $h^e(t)$, which is used during the signal recovering process the following N_b data transmissions.

2.3.2 Zero Forcing Frequency Domain Equalization

The estimation of the wireless channel can then be used by various techniques to recover the received signal. One such technique is zero forcing frequency domain equalization (ZF-FDE), which simply multiplies the received signal $R(n)$ with an equalization weight $w(n)$ to retrieve the equalized received signal as

$$\hat{R}(n) = R(n)w(n) \tag{2.6}$$

for the nth frequency [1]. The equalization weight $w(n)$ is the multiplicative inverse of the estimated channel gain expressed by

$$w(n) = \frac{H^*(n)}{|H(n)|^2} \tag{2.7}$$

where $H^*(n)$ is the conjugate of $H(n)$ [1]. ZF-FDE overcomes the problem with intersymbol interference, but amplifies the noise. How ZF-FDE is applied in this work is described in Chapter 4.

2.4 Orthogonal Frequency Division Multiplexing

Orthogonal frequency division multiplexing (OFDM) is a multi-carrier modulation technique which divides the carrier frequency into several sub carriers, where each sub carrier can be used to send one symbol at a time [16]. The orthogonality is the result of all sub carriers being separated at very precise frequencies which is needed to avoid interference between different sub carriers. A system using OFDM is less sensitive to frequency-selective fading because of the signal being transmitted over several different frequencies. OFDM systems are also less sensitive to intersymbol interference (ISI), which is a problem with high bit rates, since the bit rate stream is split into many parallel streams with lower bit rate. ISI is the result of one transmission interfering with the following transmission because of delayed signals due to multipath fading.

Figure 2.6 illustrates an OFDM transmission system [1]. The main part of an OFDM system is the use of IFFT and FFT. The transmitter, shown in Fig. 2.6(a), uses an N_c-point IFFT to divide the data onto N_c sub carriers and the receiver, shown in Fig. 2.6(b), applies an N_c-point FFT to the received signal to recombine it into one signal.

2.4.1 Guard Interval

The purpose of using cyclic prefix (CP) or guard interval (GI) in an OFDM system, as illustrated in Fig. 2.6 (GI insertion and GI removal), is to prevent ISI even further. A

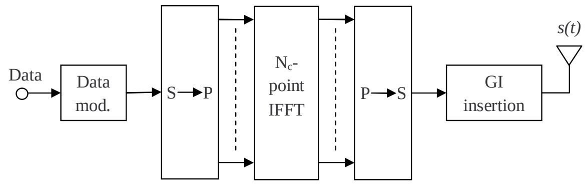

(a) In the transmitter the data is modulated, sent through an N_c-point IFFT and then transmitted after GI insertion.

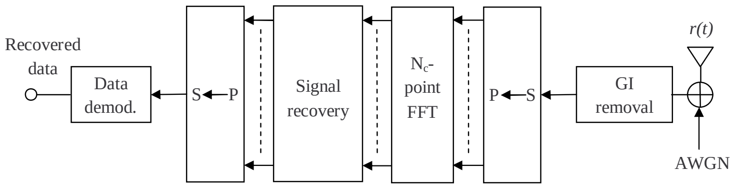

(b) When the signal is received at the receiver, it removes the GI, passes it through an N_c-point FFT, performs signal recovery and then demodulates the signal to retrieved the data represented by the signal.

Figure 2.6: The transmitter and receiver in an OFDM system [1]

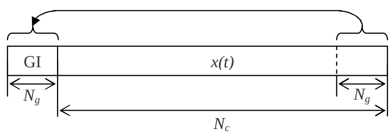

Figure 2.7: Guard interval insertion: The last N_g symbols of the signal are copied and inserted at the beginning of the signal.

GI of length N_g is copied from the end and inserted at the beginning of each transmission as shown in Fig. 2.7. If the GI is longer than the maximum multipath delay spread the problem with ISI can be avoided. The downside with using a GI is the overhead that could have been used to transmit data instead [19].

2.5 Analog Network Coding

Consider the situation illustrated in Fig. 2.8, where user U_0 and U_1 want to exchange information with each other in a wireless network. The channel between them is assumed to be half duplex, so two stages are required for them to exchange information.

Now consider the situation where an obstacle has been placed between user U_0 and U_1 so they no longer can communicate directly with each other. To solve this problem, the relay R is added to the network, as illustrated in Fig. 2.9, through which the users can transmit their data to reach each other. A network of this kind is called a two-way relay network (TWRN). In this situation, four stages are needed instead of the two required by the original situation, which is a system performance degradation of 50%.

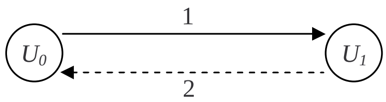

Figure 2.8: A two-way network where the users, U_0 and U_1, exchanges data during two stages.

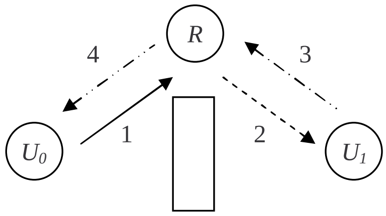

Figure 2.9: A two-way relay network where the users, U_0 and U_1, use four stages to exchange data.

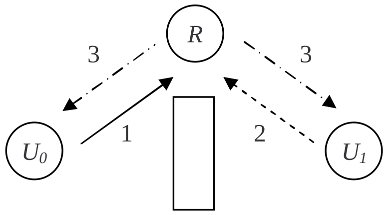

Figure 2.10: A two-way relay network with digital network coding. The number of stages needed for the users, U_0 and U_1, to exchange data is reduced from four to three.

2.5.1 Digital Network Coding

When a signal is transmitted in a wireless network, it will be received by all users within the reach of the signal. This is due to the natural broadcasting ability of the wireless medium, which has always been treated as a problem because if two users transmit at the same time their signals will interfere with each other. The broadcasting capability can however be exploited to increase the network throughput in a TWRN when combined with some simple processing in the relay [3]. If the relay is given the capability to mix two data packets together, the original four stages needed in the TWRN to exchange data can be reduced to three stages as illustrated in Fig. 2.10. User U_0 and U_1 transmit their packets D_0 and D_1 during the first and second stage, respectively. The relay receives the data packets, uses bitwise exclusive OR (XOR) as $D_0 \bigoplus D_1 = D_{0,1}$ to combine the two packets into one and then broadcasts it to the users during the third stage [20]. The data packet sent from the other user $\bar{j}$, where $\{j = 0, 1\}$, can now be retrieved at user j by bitwise XOR as $\{D_j \bigoplus D_{0,1} = D_{\bar{j}}\}$. This is called digital network coding.

2.5.2 Analog Network Coding

Physical-layer network coding (PNC) was introduced in [5], which exploits the broadcasting capabilities of the wireless medium even further by allowing both users in a TWRN to

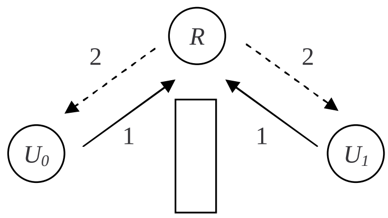

Figure 2.11: A two-way relay network with physical-layer network coding. Only two stages are necessary for the users, U_0 and U_1, to exchange data.

transmit at the same time. With this approach only two stages are needed to exchange data between two users as illustrated in Fig. 2.11. The first stage is used by the users to transmit to the relay and the second stage is used by the relay to broadcast the combined signal back to the users. PNC does however require the use of decode-and-forward, which makes the relay more complex. If decode-and-forward is used the relay have to decode the received signal, re-encode it and forward it.

Recently, analog network coding (ANC) was introduced, which is a less complex version of PNC, where the relay uses amplify-and-forward instead of decode-and-forward [7]. The amplify-and-forward protocol is less complex because no decoding is done in the relay, the signal is only amplified and forwarded. ANC is described in detail in Chapter 3.

Chapter 3

The Network Model

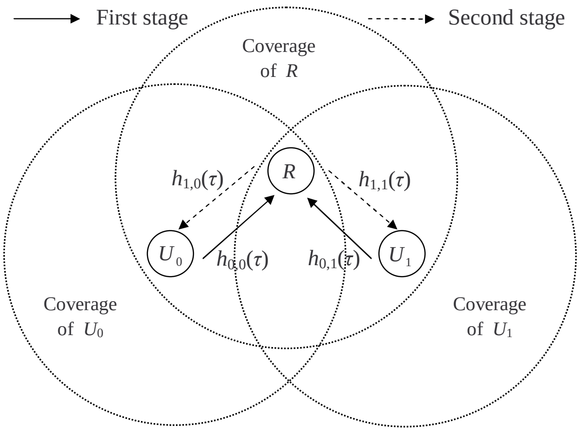

Figure 3.1: A wireless network consisting of the users, U_0 and U_1, and the relay R. The users communicate with each other through the relay in two stages.

The network model considered in this work is the two-way relay network shown in Fig. 3.1, which consists of the two users, U_0 and U_1, and the relay Ro. The channel is half duplex which means that the users and the relay cannot communicate with each other at the same time and thus, the communication process is divided into two stages. During the first stage the users U_0 and U_1 transmit their respective signals to the relay, and in the second stage the relay broadcast the received signal to the users following an amplify-and-forward protocol.

Before the communication process starts, the jth user U_j generates a data-modulated symbol sequence which can be represented by $\{d_j(n); n = 0 \sim N_c - 1\}$. The symbol sequence is then fed to an N_c-point inverse fast Fourier transform (IFFT) function to generate a time domain OFDM signal with N_c subcarriers represented as [21]

$$s_{0,j}(t) = \sqrt{P} \sum_{n=0}^{N_c-1} d_j(n) \exp\left(j2\pi t \frac{n}{N_c} \right), \tag{3.1}$$

for $t = 0 \sim N_c - 1$, where P $(= E_s/T_c N_c)$ is the power coefficient (E_s and T_c denotes the data-modulated symbol energy and the sampling period of IFFT, respectively). An N_g-

samples guard interval (GI) is inserted at the beginning of the signal to prevent interference from earlier transmitted signals. Finally, both users transmit their respective signal at the same time to the relay over a multipath fading channel.

The propagation channel can be expressed by the discrete-time channel impulse response given by

$$h_{m,j}(\tau) = \sum_{l=0}^{L-1} h_{l,m,j}\delta(\tau - \tau_l), \tag{3.2}$$

where L, $h_{l,m,j}$, τ_l and $\delta(\tau - \tau_l)$ denotes the number of paths, the path gain between the jth user U_j and the relay during the mth stage, the time delay of the lth path and the delta function, respectively.

3.1 First Stage

After GI removal, the signal received at the relay can be expressed by

$$r_r(t) = \sum_{l=0}^{L-1}\sum_{j=0}^{1} h_{l,0,j}s_{0,j}(t - \tau_l) + n_r(t) \tag{3.3}$$

for $t = 0 \sim N_c - 1$, where $s_{0,j}(t - \tau_l)$, $h_{l,0,j}$ and $n_r(t)$ are the jth users transmitted signal received with time delay τ_l, the path gain between user U_j and the relay at the first stage and the additive white Gaussian noise (AWGN), respectively.

3.2 Second Stage

The relay amplifies the received signal by a factor of $\sqrt{P}$ expressed by

$$\tilde{r}_r(t) = \sqrt{P}r_r(t) \tag{3.4}$$

for $t = 0 \sim N_c - 1$. An N_c-samples GI is inserted at the beginning of signal. $\tilde{r}_r(t)$ is then broadcasted to both users.

After GI removal, the time domain signal received at the jth user U_j can be expressed as

$$r_j(t) = \sum_{l=0}^{L-1}\sum_{j=0}^{1} h_{l,1,j}\tilde{r}_r(t - \tau_l) + n_j(t) \tag{3.5}$$

for $t = 0 \sim N_c - 1$, where $\tilde{r}_r(t - \tau_l)$, $h_{l,1,j}$ and $n_j(t)$ are the relay's broadcasted signal received with time delay τ_l, the path gain between the relay and user U_j during the second stage and the AWGN, respectively.

$r_j(t)$ is then fed to an N_c-point fast Fourier transform (FFT) function to transform it into the frequency domain signal expressed as

$$R_j(n) \;=\; \tilde{R}_r(n)H_{1,j}(n) + N_j(n) \tag{3.6}$$

for $n = 0 \sim N_c - 1$, where $\tilde{R}_r(n)$, $H_{1,j}(n)$ and $N_j(n)$ represents relay's broadcasted signal, the channel gain between the jth user U_j and the relay during the second stage and the AWGN.

To recover the signal transmitted by the partner user $U_{\bar{j}}$, user U_j has to remove its self-information (the signal sent by user U_j during the first stage) and carry out one-tap zero forcing frequency domain equalization (ZF-FDE). First, user U_j removes its self-information at the nth subcarrier as [8]

$$\tilde{R}_j(n) = R_j(n) - d_j(n)H_{0,j}(n)H_{1,j}(n) \tag{3.7}$$

for $n = 0 \sim N_c - 1$. Secondly, one-tap ZF-FDE is applied as

$$\hat{R}_j(n) = \tilde{R}_j(n)w_j(n), \tag{3.8}$$

where the jth user U_j equalization weight $w_j(n)$, is given by [8]

$$w_j(n) = \frac{H^*_{0,\bar{j}}(n)H^*_{1,j}(n)}{|H_{0,\bar{j}}(n)H_{1,j}(n)|^2}. \tag{3.9}$$

In eq. (3.9), $(\cdot)^*$ denotes the complex conjugate operation and the bar over j signifies the unitary complement operation (i.e. "NOT" operation) that performs logical negation of j.

Note here that the estimates of the channel gains are needed to perform self-information removal and one-tap ZF-FDE given by eqs. (3.7) and (3.9), respectively. The channel gains $\{H_{0,j}(n)\}$ and $\{H_{1,j}(n)\}$ are replaced by the channel gain estimates $\{H^e_{0,j}(n)\}$ and $\{H^e_{1,j}(n)\}$, respectively, when channel estimation has been performed as described in Chapter 4.

Chapter 4

Channel Estimation

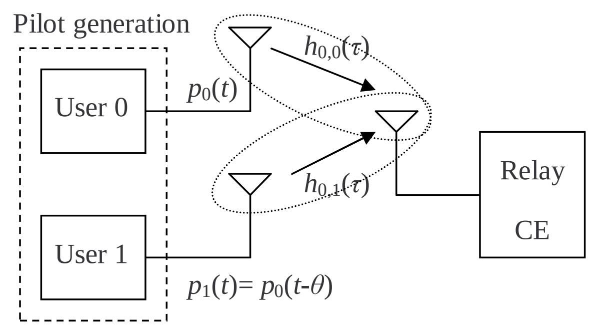

(a) MISO system: The users transmit their respective pilot signal, $p_0(t)$ and $p_1(t)$, to the relay during the first stage.

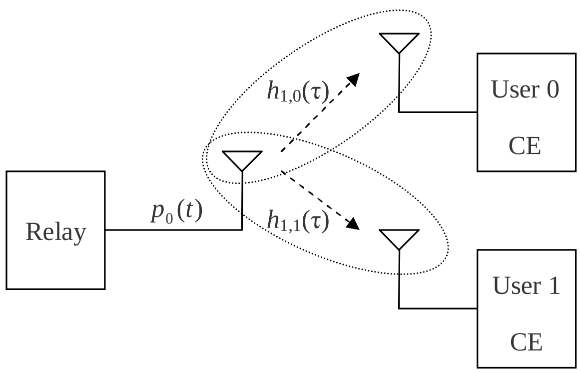

(b) Two independent SISO systems: The relay broadcast its pilot signal, $p_0(t)$, to both users during the second stage.

Figure 4.1: The proposed CE scheme represented as one MISO system and two SISO systems.

The pilot-assisted channel estimation (CE) scheme for ANC network presented in this work is divided into two stages similar to the two stages described in Chapter 3. During the first stage, the users transmit their respective pilot signals to the relay, and during the second stage the relay broadcasts its pilot signal to the users. These two stages can be represented as different systems; one multiple-input single-output (MISO) system during the first transmission stage and two independent single-input single-output (SISO) systems during the second transmission stage. The first stage of the CE process can be described as a MISO-CE system since the pilot signals from both users' antennas are received by the relay's single antenna, as illustrated in Fig. 4.1a. The second stage of the CE process, illustrated in Fig. 4.1b, can be described as two independent SISO-CE systems since the relay's pilot signal is broadcasted by a single antenna at the relay while the pilot signal is received by each user's antenna independently.

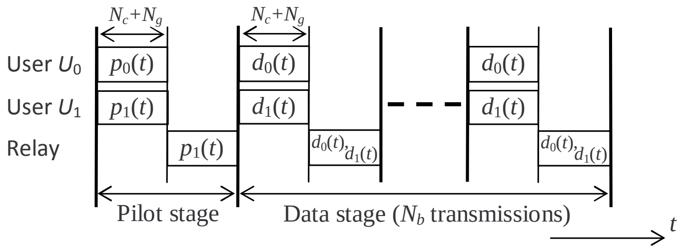

Figure 4.2: The transmission structure consists of one pilot transmission stage followed by N_b data transmission stages.

Figure 4.2 illustrates the relationship between pilot and data transmissions and how they are carried out by the different terminals in the network. The pilot transmission stage consists of two time slots where each time slot has a length of $N_c + N_g$ samples, where N_c is the number of OFDM sub carriers and N_g is the length of the guard interval. The first time slot during the pilot transmission stage corresponds to the first CE stage which is used to transmit the pilot signals, $p_0(t)$ and $p_1(t)$ from the users U_0 and U_1, respectively. The second time slot of the pilot transmission stage is used by the relay during the second CE stage to broadcast its pilot signal $p_0(t)$ to the users U_0 and U_1. A pilot transmission stage is followed by N_b data transmission stages each divided into two time slots. The first and the second time slot of a data transmission stage correspond to the first and second stage described in Chapter 3, respectively.

4.1 First Stage

During the first stage of the CE process the users, U_0 and U_1, transmit their pilot signals, $p_0(t)$ and $p_1(t)$, respectively, to the relay. The pilot signal $p_1(t)$ transmitted by U_1 is cyclicly shifted relative to the pilot signal $p_0(t)$ transmitted by U_0. $\{p_1(t) = p_0(t-\theta); t = 0 \sim N_c-1\}$, where θ denotes the cyclic shift. By transmitting pilot signals designed this way, the problem of overlapping channel impulse responses from different users can be avoided at the relay and both CSIs of the channels between the users and the relay can be estimated as presented next.

After GI removal the received time domain pilot signal at the relay can be expressed as

$$
\begin{aligned}
r_r(t) &= \sum_{l=0}^{L-1}\sum_{j=0}^{1} h_{l,0,j}p_j(t-\tau_l) + n_r(t) \\
&= \sum_{l=0}^{L-1} h_{l,0,0}p_0(t-\tau_l) + \sum_{l=0}^{L-1} h_{l,0,1}p_0(t-\tau_l)\exp\bigg(-j2\pi\theta\frac{n}{N_c}\bigg) + n_r(t) \qquad (4.1)
\end{aligned}
$$

for $t = 0 \sim N_c - 1$, where $p_j(t-\tau_l)$, $h_{l,0,j}$ and $n_r(t)$ are the jth users transmitted pilot signal received with time delay τ_l, the path gain between user U_j and the relay during the first CE stage and the additive white Gaussian noise (AWGN), respectively. We used the time shifting property of Fourier transform applied to $\{p_1(t) = p_0(t-\theta); t = 0 \sim N_c - 1\}$ [15]. N_c-point FFT is applied to transform the received signal into the frequency domain signal represented by

$$
\begin{aligned}
R_{r,p}(n) &= P_0(n)H_{0,0}(n) \\
&+ P_0(n)H_{0,1}(n)\exp\bigg(-j2\pi\theta\frac{n}{N_c}\bigg) \\
&+ N_r(n) \qquad (4.2)
\end{aligned}
$$

for $n = 0 \sim N_c - 1$. The estimate of the channel gain is obtained by reverse modulation as

$$
\begin{aligned}
H_{r,e}(n) &= \frac{R_{r,p}(n)}{P_0(n)} \\
&= H_{0,0}(n) + H_{0,1}(n)\exp\bigg(-j2\pi\theta\frac{n}{N_c}\bigg) \\
&+ \tilde{N}_r(n) \qquad (4.3)
\end{aligned}
$$

for $n = 0 \sim N_c - 1$, where $P_0(n) = \mathrm{FFT}\{p_0(t)\}$ and $\tilde{N}_r(n) = N_r(n)/P_0(n)$. Then, N_c-point IFFT is applied to transform the estimated channel gain into the estimated channel impulse response $\{h_{r,e}(\tau); \tau = 0 \sim N_c - 1\}$, which is illustrated in Fig. 4.3(a). A filter is used to separate the two channel gains, $h^e_{0,0}(\tau)$ and $h^e_{0,1}(\tau)$, as

$$
h^e_{0,0}(\tau) = \begin{cases} h^e_0(\tau), & \text{where } \tau = 0 \sim N_g - 1, \\ 0, & \text{elsewhere.} \end{cases} \qquad (4.4)
$$

and

$$
h^e_{0,1}(\tau) = \begin{cases} h^e_0(\tau-\theta), & \text{where } \tau = \theta \sim \theta + N_g - 1, \\ 0, & \text{elsewhere,} \end{cases} \qquad (4.5)
$$

as illustrated in Figs. 4.3(b) and 4.3(c), respectively. Note that the estimate of the channel impulse response $h_{0,1}(\tau)$ in eq. (4.5) is shifted by θ.

Finally, to obtain the estimates of the channel gains, $\{H^e_{0,0}(n); n = 0 \sim N_c - 1\}$ and $\{H^e_{0,1}(n); n = 0 \sim N_c - 1\}$ between the relay and the users, an N_c-point FFT is applied to both $\{h^e_{0,0}(\tau)\}$ and $\{h^e_{0,1}(\tau)\}$. Note that the estimated channel gains, $\{H^e_{0,0}(n)\}$ and $\{H^e_{0,1}(n)\}$, are not used by the relay but by the users U_0 and U_1. Hence, the channel gains have to be sent from the relay to the users. However, how the channel gains are transmitted to the users from the relay is not in the scope of this work, and thus, it is assumed that they are transmitted to both users by a higher layer protocol.

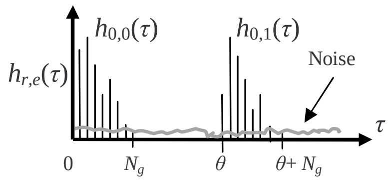

(a) Estimated channel impulse response $h_{r,e}(\tau)$.

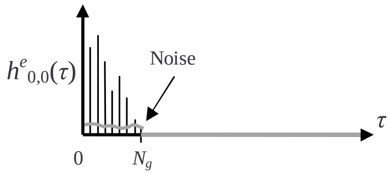

(b) $h_{r,e}(\tau)$ after filtering by eq. (4.4).

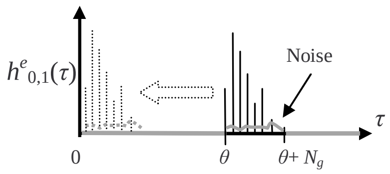

(c) $h_{r,e}(\tau)$ after filtering by eq. (4.5).

Figure 4.3: Separation of the channel impulse responses ($h^e_{0,0}$ and $h^e_{0,1}$ between the relay and both users, U_0 and U_1, during the first transmission stage).

4.2 Second Stage

The relay amplifies its pilot signal, $p_0(t)$, by a factor of $\sqrt{P}$ and broadcast it as

$$\tilde{p}_0(t) = \sqrt{P} p_0(t) \tag{4.6}$$

for $t = 0 \sim N_c - 1$, during the second stage to the users U_0 and U_1. Without loss of generality we focus on CE performed by the user U_j for $j \in \{0, 1\}$ as presented below.

After GI removal, the time domain pilot signal received at the jth user U_j can be represented by

$$r_{j,p}(t) = \sum_{l=0}^{L-1} h_{l,1,j} \tilde{p}_0(t - \tau_l) + n_j(t) \tag{4.7}$$

for $n = 0 \sim N_c - 1$, where $\tilde{p}_0(t - \tau_l)$, $h_{l,1,j}$ and $n_j(t)$ are the relay's broadcasted pilot signal received with time delay τ_l, the path gain between the relay and user U_j during the second CE stage and the AWGN, respectively.

N_c-point FFT is applied to $r_{j,p}(t)$ to transform it into the frequency domain as

$$R_{j,p}(n) = \tilde{P}_0(n) H_{1,j}(n) + N_j(n) \tag{4.8}$$

for $n = 0 \sim N_c - 1$. The channel gain estimate $\{H^e_{1,j}(n); n = 0 \sim N_c - 1\}$ is obtained by reverse modulation as

$$H^e_{1,j}(n) = \frac{R_{j,p}(n)}{P_0(n)} = H_{1,j}(n) + \tilde{N}_j(n) \tag{4.9}$$

for $n = 0 \sim N_c - 1$, where $j \in \{0, 1\}$ and $\tilde{N}_j(n) = N_j(n)/P_0(n)$. Then, N_c-point IFFT is applied to $\{H^e_{1,j}(n)\}$, to obtain the time domain channel impulse response $\{h^e_{1,j}(\tau); \tau = 0 \sim N_c - 1\}$. A filter is applied to $\{h^e_{1,j}(\tau)\}$ as

$$h^e_{1,j}(\tau) = \begin{cases} h^e_{1,j}(\tau), & \text{where } \tau = 0 \sim N_g - 1, \\ 0, & \text{elsewhere.} \end{cases} \tag{4.10}$$

Finally, N_c-point FFT is applied to $\{h^e_{1,j}(\tau)\}$ as

$$H^e_{1,j}(n) = \sum_{\tau=0}^{N_g-1} h^e_{1,j}(\tau) \exp\left(- j2\pi n \frac{\tau}{N_c} \right) \tag{4.11}$$

for $n = 0 \sim N_c - 1$, to obtain the improved channel gain estimate between the relay and the jth user U_j during the second stage.

After receiving the channel gains $\{H^e_{0,0}(n)\}$ and $\{H^e_{0,1}(n)\}$ estimated at the relay, user U_0 and U_1 now have the channel gains required ($\{H^e_{0,0}(n)\}$, $\{H^e_{0,1}(n)\}$ and $\{H^e_{1,j}(n); j \in \{0, 1\}\}$) to remove self-information and detect the signal from the partner user as described in section 3.2.

Chapter 5

Results

In this chapter the simulation environment and results from the computer simulations are shown and discussed. Section 5.2 discusses the bit-error-rate (BER) performance when N_b changes and in Section 5.3, the impact of channel time-selectivity is discussed.

5.1 Simulation Environment

Table 5.1: Simulation parameters.

Transmitter (U_0, U_1)	Block size	$N_c = 256$
	GI	N_g=32
	Data modulation	QPSK
Channel	L-path block Rayleigh fading with Δ=1	
Relay	Protocol	Amplify-and-forward
	Feedback	Perfect
Receiver (U_0, U_1)	FDE	ZF
	Channel estimation	Pilot-assisted

The simulation environment parameters are summarized in Table 5.1. We assume the OFDM system with $N_c = 256$-subcarriers, $N_g = 32$ and ideal coherent quadrature phase shift keying (QPSK) modulation and demodulation with $E[|d_j(n)|^2] = 1$. The propagation channel is $L = 16$-path block Rayleigh fading channel, where $\{h_{l,m,j}; l = 0 \sim L-1\}$ are zero-mean independent complex variables with $E[|h_{l,m,j}|^2] = 1/L$. We assume $\tau_0 = 0 < \tau_1 < \cdots < \tau_{L-1}$ and that the lth path time delay is $\tau_l = l\Delta$, where Δ (≥ 1) is the time delay separation between the previous and following path. The maximum time delay spread of the channel is less than the GI length and all paths are independent of each other. $f_D T_s$ denotes the normalized maximum Doppler frequency,where $1/T_s = 1/[T_c(1 + N_g/N_c)]$ is the transmission symbol rate ($f_D T_s = 10^{-4}$ corresponds to a mobile terminal speed of approximately 19 km/h for a transmission data rate of 100 Msymbols/s and a carrier frequency of 2GHz). We assume neither shadowing nor path loss and ideal feedback channel between the relay and the users. As a pilot we use a Chu-sequence given by $\{p_0(t) = \exp\{j\pi t^2/N_c\}; t = 0 \sim N_c - 1\}$ [22].

All simulations were run on a small inofficial cluster, called master 4, located in Professor Adachi's laboratory [13].

5.2 BER Performance

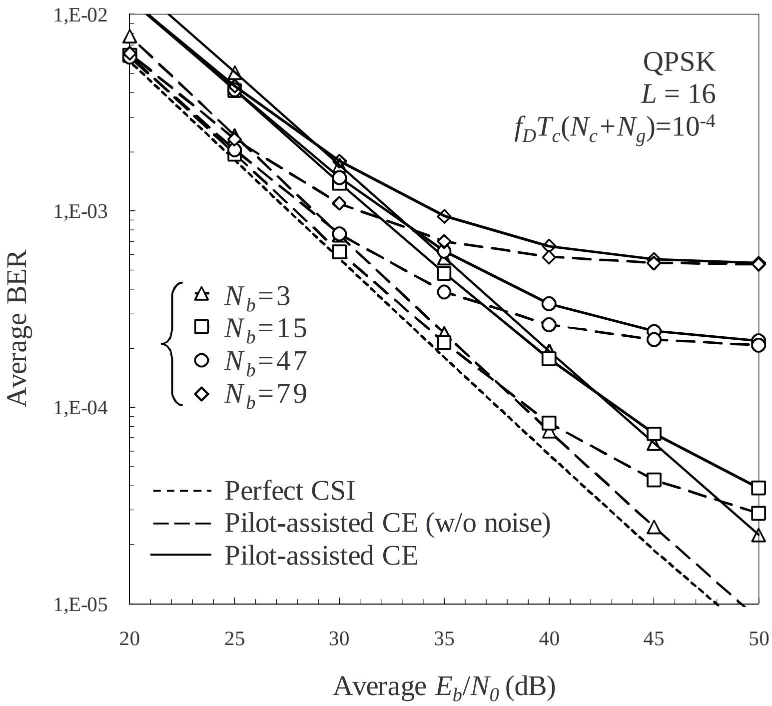

Figure 5.1: BER performance.

The results from the first simulation, illustrated in Figure 5.1, shows the BER performance as a function of the average signal energy per bit-to-AWGN power spectrum density ratio $E_b/N_0(= 0.5 \times (E_s/N_0) \times (1 + N_g/N_c) \times (1 + 1/N_b))$ for $N_b = 3$, 15, 47, and 79. The power loss due to GI and pilot insertion are taken into consideration. We note here that the terms "Perfect CSI" and "Pilot assisted CE (w/o noise)" in Fig. 5.1, respectively, denote the perfect knowledge of CSI at all terminals and pilot-assisted CE without the noise effect during the estimation process (only tracking errors due to channel time selectivity are taken into consideration).

It can be seen in figure 5.1 that the BER performance of the proposed channel estimator for broadband ANC degrades in comparison with the perfect CSI case; for BER $= 10^{-3}$ the E_b/N_0 degradation is about 5, 4, 4.5, and 7 dB when $N_b = 3$, 15, 47, and 79, respectively. In the case of CE w/o noise (long-dotted lines in Fig. 5.1), where only the propagation errors due to channel time selectivity are considered, for BER $= 10^{-3}$, the E_b/N_0 degradation is about 3.5, 3.7, 3.8 and 4 when N_b =3, 15, 47 and 79, respectively.

It can also be seen from the figure that as the number of data frames N_b increases, the BER performance slightly improves in comparison with the case of $N_b = 3$ when $E_b/N_0 < 29$ dB. This is because of lower power loss due to a lower frequency of pilot insertions. However, it can be seen that the BER performance does not improve anymore for $N_b \geq 16$ when E_b/N_0

is small. This is because further increase of N_b (increased data power due to lower frequency of pilot insertion) cannot overcome the errors caused by noise.

On the other side, it can be seen that the $N_b = 3$ case is starting to perform better than N_b =15, 47 and 79 when $E_b/N_0 = 42$, 33.5 and 29 dB, respectively. This is because a more frequent pilot insertion (a lower N_b) has a better tracking ability against the channel fading variations; In the case of $N_b = 47$ and 79 a BER floor of about 2×10^{-4} and 5×10^{-4}, respectively, is observed since in the case of larger N_b the channel estimation at the beginning of the frame and the actual channel gain at the end differs and causes the channel propagation errors.

5.3 Impact of Channel Time-selectivity

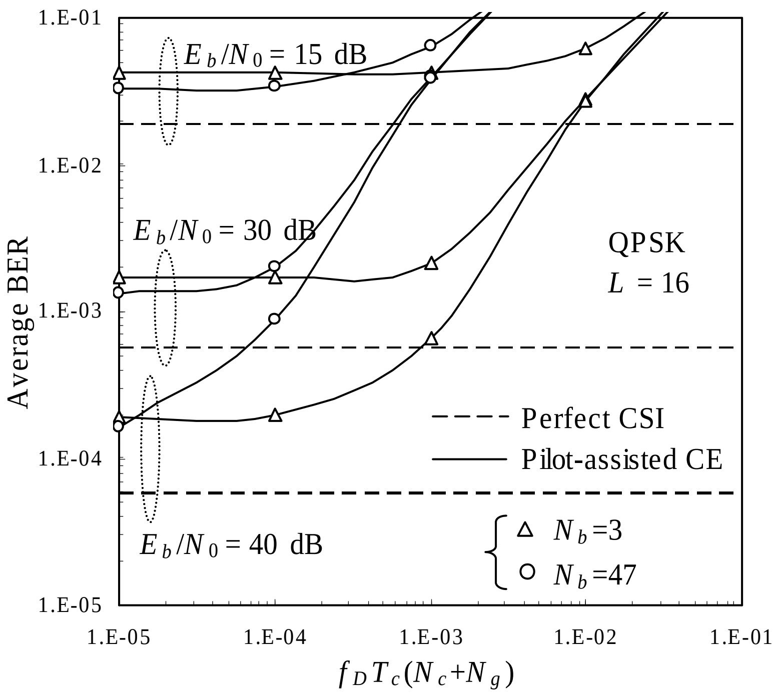

Figure 5.2: Impact of $f_D T_s$.

The results from the second simulation shows the impact of $f_D T_s$ on the BER performance with practical CE. When $f_D T_s$ increases (the transmission symbol rate and mobile speed from Section 5.2 are used and kept constant), the tracking ability against the multipath fading variations tends to be lost. Figure 5.2 illustrates the BER performance as a function of $f_D T_s$ for $E_b/N_0 = 15$ dB, 30 dB and 40 dB with $N_b = 3$ and 47. The dotted lines in the graphs represent the BER performance of pilot-assisted CE without the noise effect.

Figure 5.2 shows that when $f_D T_s = 10^{-5}$, the BER performance is close to equal irrespectively of N_b for all E_b/N_0 cases. $f_D T_s = 10^{-5}$ corresponds to a mobile terminal speed of about 2 km/h, which only causes low variations in the channel. If the speed of the mobile terminal is increased to about 19 km/h resulting in $f_D T_s = 10^{-4}$, we start to see the impact of $f_D T_s$ on the BER performance, especially for $N_b = 47$ in the $E_b/N_0 = 40$ dB case. If the speed is increased even more to about 190 km/h, which corresponds to $f_D T_s = 10^{-3}$, the channel fading effect becomes even more obvious, and for $N_b = 47$ the BER performance is severely degraded because the tracking ability of the channel estimator against the channel time selectivity is lost.

Chapter 6

Conclusions

In this thesis we have presented a pilot-assisted CE scheme for broadband ANC, which maintains the capacity benefits of ANC by only using two stages to estimate all CSIs in the network. During the first stage the users transmit their pilot signals to the relay, and during the second stage the relay broadcast its pilot signal to both users. To overcome the problem with overlapping pilots during the first stage at the relay, one of the users transmit a cyclically shifted pilot signal.

The proposed pilot-assisted CE scheme was evaluated by computer simulations, were the BER performance and the impact of channel time-selectivity were examined. Our results show that the BER performance of broadband ANC with practical CE gives a satisfactory performance for a low and moderate mobile terminal speed in a multipath fading channel. The results also show that a high terminal speed severely degrades the BER performance which makes the choice of pilot insertion interval very important.

6.1 Future Work

One important problem is the feedback of the estimated CSIs at relay terminal to the users, which is vital in practical CE. This was not considered in this thesis, but is left as future interesting work.

Chapter 7

Acknowledgements

First of all I want to thank Professor F. Adachi for accepting me into his laboratory and for all the constructive input I have gotten from him during this project. I also want to thank Dr. H. Gacanin for all the help he has been giving me from idea to having a finished thesis report. Without him I could not have done this project. Finally I want to thank my internal supervisor Jerry Eriksson for his comments during the final stage of the project.

References

[1] H. Gacanin. Ofdm/tdm transmission technique for broadband mobile radio. master's thesis. Technical report, Dept. of Electrical and Communication Engineering, Tohoku University, Sendai, Japan, 2005.

[2] R. W. Yeung. Multilevel diversity coding with distortion. *IEEE Trans. Inform. Theory*, IT-41:412–422, 1995.

[3] S.-Y. R. Li R. W. Yeung R. Ahlswede, N. Cai. Network information flow. *IEEE Trans. Inform. Theory*, 46:1204–1216, 2000.

[4] R. W. Yeung S.-Y. R. Li and N. Cai. Linear network coding. *IEEE Trans. Inform. Theory*, 49:371–381, 2003.

[5] S.-C. Liew S. Zhang and P. Lam. Hot topic: Physical layer network coding. *ACM The 12th MobiCom 2006*, pages 358–365, 2006.

[6] P. Popovski and H. Yomo. Bi-directional amplification of throughput in a wireless multi-hop network. *IEEE 63rd Vehicular Technology Conference (VTC)*, 2006.

[7] S. S. Gollakota S. Katti and D. Katabi. Embracing wireless interference: Analog network coding. Technical report, MIT Tech., Cambridge, England, 2007.

[8] H. Gacanin and F. Adachi. Performance of physical layer network coding in a frequency-selective fading channel. *IEEE International Symposium on Personal, Indoor and Mobile Radio Communications (PIMRC'09)*, 2009.

[9] A. Puri S. Coleri, M. Ergen and A. Bahai. Channel estimation techniques based on pilot arrangement in ofdm systems. *IEEE Trans. on Comm.*, 48:362–370, 2002.

[10] K. Berberidisi A. Lalos, A.A. Rontogiannis. Channel estimation techniques in amplify and forward relay networks. *Proc. IEEE Workshop on Signal Processing Advances in Wireless Communications (SPAWC)*, 2008.

[11] J. H. Winters Y. (G.) Li and N. R. Sollenberger. Simplified channel estimation for ofdm systems with multiple transmit antennas. *IEEE Trans. on Comm.*, 1:67–75, 1999.

[12] R. Zhang F. Gao and Y-C. Liang. On channel estimation for amplify-and-forward two-way relay networks. *IEEE Global Communication Conference (Globecom'08)*, 2008.

[13] Professor F. Adachi's Laboratory.
http://www.mobile.ecei.tohoku.ac.jp/adachi-e/index.html (visited 2009-10-09).

[14] T. Sjödin H. Gacanin and F. Adachi. Two-slot channel estimation for analog network coding based on ofdm in a frequency-selective fading channel. *2010 IEEE 71th Vehicular Technology Conference (VTC2010-Spring)*, 2010.

[15] Dimitris G. Manolakis John G. Proakis. *Digital Signal Processing*. Pearson Prentice Hall, Upper Saddle River, New Jersey, 2007.

[16] J. Schiller. *Mobile Communications*. Addison-Wesley, Boston, 2003.

[17] M. Pueschel M. Frigo-S. G. Johnson C. S. Burrus, I. Selesnick. *Fast Fourier Transforms*. 2009. http://cnx.org/content/col10550/1.20 (visited 2009-10-15).

[18] B. Sklar. Rayleigh fading channels in mobile digital communication systems - part i. *IEEE Commun. Mag.*, 35:136–146, 1997.

[19] P. Viswanath D. Tse. *Fundamentals of Wireless Communication*. Cambridge University Press, 2005. http://www.ifp.illinois.edu/ pramodv/book.html (Chapter 5, visited 2009-10-16).

[20] S. Y. Kung Y. Wu, P. A. Chou. Information exchange in wireless networks with network coding and physical layer broadcast. Technical report, Microsoft Research, Redmond WA, 2004.

[21] S. Hara and R. Prasad. *Multicarrier Techniques for 4G Mobile Communications*. Artech House Publishers, 2003.

[22] D. C. Chu. Polyphase codes with good periodic correlation properties. *IEEE Trans. on Inf. Theory*, 4:531–532, 1972.